

Complex stellar populations in massive clusters: trapping stars of a dwarf disc galaxy in a newborn stellar super-cluster

M. Fellhauer^{1,3} [★], P. Kroupa^{2,3} [†] and N. W. Evans¹ [‡]

¹ Institute of Astronomy, University of Cambridge, Madingley Road, Cambridge CB3 0HA, UK

² Argelander Institute for Astronomy, University of Bonn, Auf dem Hügel 71, D-53121 Bonn, Germany

³ The Rhine Stellar-Dynamical Network

21 September 2017

ABSTRACT

Some of the most massive globular clusters of our Milky Way, such as for example ω -Centauri, show a mixture of stellar populations spanning a few Gyr in age and 1.5 dex in metallicities. In contrast, standard formation scenarios predict that globular and open clusters form in one single star-burst event of duration $\lesssim 10$ Myr and therefore should exhibit only one age and one metallicity in its stars. Here, we investigate the possibility that a massive stellar super-cluster may trap older galactic field stars during its formation process that are later detectable in the cluster as an apparent population of stars with a very different age and metallicity.

With a set of numerical N-body simulations, we are able to show that, if the mass of the stellar super-cluster is high enough and the stellar velocity dispersion in the cluster is comparable to the dispersion of the surrounding disc stars in the host galaxy, then up to about 40 per cent of its initial mass can be additionally gained from trapped disc stars. We also suggest that a super-cluster may capture in excess of its own mass under certain conditions.

Key words: galaxies: dwarfs – galaxies: star clusters – methods: N-body simulations – globular clusters: individual: ω Cen

1 INTRODUCTION

The most massive globular cluster in the Milky Way, ω -Centauri, ($5 \times 10^6 M_{\odot}$, Meylan et al. 1995) is also one of the most enigmatic of star clusters. It shows a spread in stellar populations in age (≈ 3 –5 Gyr) and metallicity ($-2.0 \lesssim [\text{Fe}/\text{H}] \lesssim -0.5$) (e.g. Hilker & Richtler 2000; Norris & Da Costa 1995) with metal-poorer stars having a less-concentrated radial distribution than the more metal-rich population (van Leeuwen et al. 2000). The metal-poorer population also rotates with a maximum rotation speed of 8 km s^{-1} (Freeman 2001), whereas the more metal-rich population does not (e.g. Norris et al. 1997). Seventy per cent of the population of ω Cen have a metallicity of $[\text{Fe}/\text{H}] \approx -1.7$, 25 per cent have $[\text{Fe}/\text{H}] \approx -1.2$ while 5 per cent have $[\text{Fe}/\text{H}] \approx -0.7$ (Hilker & Richtler 2000). The cluster¹ orbits the Milky Way in a slightly inclined (mostly within the disc), highly eccentric (peri-galacticon ≈ 1 kpc, apogalacticon ≈ 6.4 kpc), retrograde orbit well within the Solar radius (Tsuchiya et al. 2004). Some effects of the colour-magnitude diagram (CMD) may only be explainable with an unusual helium enrichment (Bekki & Norris 2006; Piotto et al.

2005) of some stars, while other workers prefer the scenario of different distinct metallicity populations (Sollima et al. 2006).

A similar spread in metallicities is found in the most massive globular cluster G1 in M31 (Meylan et al. 2001). It is even debated if NGC 6388 and NGC 6441, two globular clusters of the Milky Way which are unusually metal rich and quite massive, also show multiple stellar populations (Ree et al. 2002).

As a possible formation scenario, some authors believe that these clusters are massive enough to retain part of their gas content, stemming from their initial formation, which then is able to cause a second episode of star formation (e.g. Platais et al. 2003). Another scenario sees these clusters as stripped cores of disrupted nucleated dwarf galaxies (e.g. Bekki & Norris 2006; Ideta & Makino 2004; Tsuchiya et al. 2004). According to a third scenario, a massive cluster may accrete co-moving inter-stellar gas from its host galaxy leading to later episodes of star-formation (Kroupa 1998). A fourth scenario proposed by Kroupa (1998) sees a massive star-cluster complex (a ‘stellar super-cluster’) forming in a tidally-driven star-burst off-centre in the host galaxy thereby capturing older and metal-poorer field stars from the host. A simple estimate shows that the captured population may be substantial if the super-cluster formation-time-scale is shorter than the field-star crossing time-scale through the forming super-cluster. Fellhauer (2004) returned to this scenario in the context of ω Cen suggesting it may have formed through merged star clusters from a star-cluster complex during the star-burst in a disrupting gas-rich dwarf galaxy as it

[★] madf@ast.cam.ac.uk

[†] pavel@astro.uni-bonn.de

[‡] nwe@ast.cam.ac.uk

¹ The relaxation time of ω Cen is close to a Hubble time and so it may be equally valid to refer to this object as being a low-mass ultra-compact dwarf galaxy (UCD).

plunged into the Milky Way. During its formation the cluster then traps stars from the underlying satellite before its disruption causing the multiple populations with different kinematics. The models by Fellhauer (2004) can reproduce the kinematics within ω Cen, but did not model the populations in the object.

Here, we investigate a more general view of the fourth scenario. The formation of a cluster complex takes about 10 Myr, which would also be the time-scale for capturing field-stars. This star-burst may have been triggered by a previous perigalacticon passage of the dwarf galaxy, but the final disruption of the host dwarf galaxy takes of the order of 100 Myr or longer being the dynamical time scale near the young Milky Way.

While on the one hand, we see massive globular clusters with multiple populations, on the other hand, we do find dwarf galaxies with off-centre nuclei (Binggeli et al. 2000). We want to investigate if these off-centre nuclei, if formed out of merged star clusters in a massive star-cluster complex inside a dwarf disc galaxy, can trap enough stars from the underlying disc such that a measurable contamination by the captured field stars with a different age and/or metallicity in the merger object may be established. The resulting off-centre massive cluster may then be stripped from its host galaxy more easily than a nucleus (i.e. in one of the perigalactica before the final destruction of the host dwarf), but the destruction of the dwarf galaxy is not part of the present work in which we concentrate on the possible capture process of field stars.

To examine our scenario, we place a massive stellar super-cluster at different radii in a dwarf disc galaxy. Note that, with this choice of these radii, our intention is to probe a parameter-space of different environments rather than to claim that these radii are actually the formation sites of the off-centre nuclei. Still, an off-centre super-cluster can later sink to the centre or at least to much lower distances from the centre (i.e. a few 100 pc as found by Binggeli et al. (2000)) due to dynamical friction. We follow the orbit of this cluster complex for a short time, i.e. the time needed to form a merger object and measure the number of disc stars which become bound to this object. A detailed description of the numerical setup will follow in the next section, while in Sect. 3 we report our results and show that under physically plausible circumstances these objects can trap as much as half of their initial mass in disc stars. I.e. one third of the stars in the final object are captured older disc stars and are not formed in the star burst which formed the object.

2 NUMERICAL SETUP

We model a dwarf disc galaxy with mass M_d , radial scale length h_0 and vertical scale height z_0 as an exponential disc in the R -direction and as isothermal sheets in the z -direction (Spitzer 1942):

$$\rho(R, z) = \rho_0 \exp(-R/h_0) \operatorname{sech}^2(z/z_0) \quad (1)$$

without a bulge. The disc is modelled 'live' using 5,000,000 particles. The disc is dynamically stable with a Toomre Q -parameter of 1.5 or higher. The surrounding dark-matter halo is modelled as an analytical logarithmic potential of the form

$$\Phi(r) = v_0^2 \ln(r^2 + R_g^2). \quad (2)$$

The newly formed super-cluster is also modelled analytically as a Plummer sphere orbiting in the disc at a radius D , with a Plummer radius $R_{\text{pl}} = 25$ pc and a total mass of M_c .

To investigate a range of parameters, we use three different

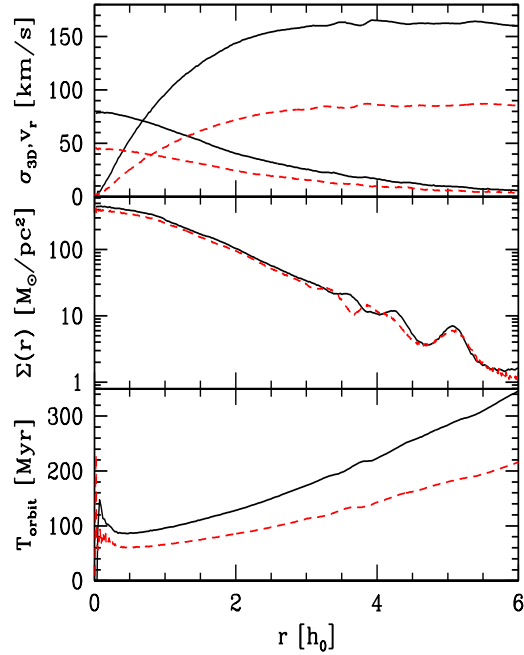


Figure 1. Properties of the two disc models. High mass disc is shown as solid lines (black on-line); low mass disc is shown as dashed lines (red on-line). Upper panel: 3D-velocity dispersion (decaying curves) and rotational velocity (increasing curves). Middle panel: Surface density of the discs. Lower panel: Orbital time, i.e. time for a star to move once around the disc.

models for the disc and two different masses for the cluster complex. In each combination of models, the distance to the centre is varied as $D = 0.5, 1.0, 2.0, 3.0$ and 5.0 scale-lengths (h_0) of the disc.

As models for the disc galaxies, we use parameters suggested by the observations of bulge-less dwarf disc-galaxies. For our low-mass galaxy we adopt parameters from NGC 3274 taken from de Blok & Bosma (2002), Swaters et al. (2002) and Swaters & Balcells (2002) – namely $M_d = 10^9 M_\odot$, $h_0 = 0.5$ kpc, $z_0 = 100$ pc, $v_0 = 80$ km s $^{-1}$ and $R_g = 1$ kpc. For our high-mass galaxy, we used $M_d = 10^{10} M_\odot$, $h_0 = 1.5$ kpc, $z_0 = 250$ pc, $v_0 = 150$ km s $^{-1}$ and $R_g = 2.5$ kpc. The third disc model has the same parameters as the first one, but with initially 10 % of the stars located in a thin, kinematically cold sub-disc with the same scale length but a maximum height of 100 pc. The radial and azimuthal velocity dispersion are artificially reduced by a factor 25 and the vertical dispersion is adjusted to the maximum height of 100 pc. The existence of such a cold population would be expected given that a substantial number of stars are born in small clusters with internal velocity dispersions $\lesssim 10$ km/s (Kroupa 2002). The velocity dispersion, rotational velocity, surface density as well as the orbital timescale of the two disc models are shown in Fig. 1.

The final mass of the super-cluster is either $10^6 M_\odot$ or $10^7 M_\odot$, and is linearly increased over a crossing-time of the super-cluster from zero to the final value at the beginning of the simulations. The crossing-times of the super-clusters are 11.7 and 3.7 Myr, respectively. The linear mass increase is chosen because it is the lowest-order approximation of a very complex process dur-

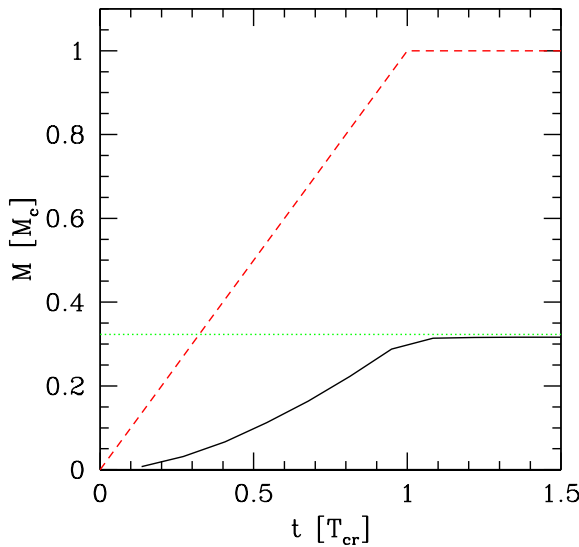


Figure 2. This figure shows the growth in mass of the super-cluster compared with the growth in mass of the trapped stars for the model with $M_d = 10^9 M_\odot$, $M_c = 10^7 M_\odot$ and $D = 1h_0$. Mass is measured in units of M_c and time in units of the crossing time (T_{cr}) of the super-cluster. Solid line (black on-line) shows the trapped stars, dashed line (red on-line) the mass of the super-cluster potential and dotted line (green on-line) the mean trapped mass determined from all data-points until 200 Myr.

ing which the gas from which the cluster-complex forms is brought together rapidly through large-scale supersonic motions. A time-resolved increase in the super-cluster potential is required as stars can only be trapped during its formation process. At later stages stars which enter the potential of the super-cluster will gain as much energy as needed to leave the cluster on the other side again. Effects like tidal capture need an interaction between the disc stars and the stars of the super-cluster and are not treated by our simple analytical treatment of the cluster potential, and are in any case extremely rare. On the other hand, it would also be unphysical to introduce the super-cluster potential instantaneously. We comment on the results from a different representation of the formation process at the end of the next section. The results are virtually indistinguishable, showing that for the trapping process it is the time-scale of the potential growth which is important, rather than the functional form of potential growth.

The simulations are carried out with the particle-mesh code Superbox (Fellhauer et al. 2000), the set-up of the grids being explained in the next section.

3 RESULTS

The super-cluster is placed at different radii, D , on a circular orbit with the circular speed at that radius. The mass of the super-cluster is increased linearly, as described above. After that, the mass of the super-cluster stays constant for the rest of the simulation. We run every model for 200 Myr and determine the number of trapped particles every 10 Myr. So even our first time slice is already after the formation of the super-cluster took place or at the very end of it. This means the trapping process is already over when we investigate the particle distribution for the first time. A particle is flagged as trapped if it has negative energy with respect to the super-cluster

potential and is located within the tidal radius of the super-cluster. We report the average number of particles bound to the cluster determined in all 20 time-slices investigated. This should ensure that the mass trapped at the formation stays approximately constant and is not just composed of 'bound' transients. Still, most disc stars are just loosely bound. This fact, as well as the choice of an analytical potential for the super-cluster, the fixed time-step (0.05 Myr) and the fixed resolution of the Superbox-grids (small disc: 17 pc within 0.5 kpc, 67 pc within 2 kpc and 267 pc beyond that; large disc: 50 pc within 1.5 kpc, 200 pc within 6 kpc and 800 pc beyond that), gives the number of bound stars in a statistical sense. We choose the 200 Myr simulation time as this is long compared to the crossing-time of the super-cluster and the time-scale on which the disc stars get trapped. This ensures that the effect of trapping stars is not a transient feature. It also spans about or more than one orbital period of the super-cluster around the disc and is the approximate time-scale between a first flyby and the final merging of a disc galaxy with another disc galaxy. But it is short compared to the time-scale the newly formed object would need to sink to the centre of the disc and form a nucleus or bulge, a process we do not study with this contribution.

The detailed trapping process during the formation of the super-cluster is not the subject of this study which concentrates on quantifying the general outcome for the first time. Basically, for a given effective potential, stars at some particular location within the final tidal radius of the super-cluster are trapped if they have a velocity too low to carry them out of the final potential of the super-cluster, and if the time-scale for the change of the potential is shorter than or comparable to their crossing time through the super-cluster. Fig. 2 plots the mass of trapped stars as a function of time (measured in crossing times of the super-cluster) in the initial period during which the super-cluster forms for the low mass disc ($M_d = 10^9 M_\odot$), massive super-cluster ($M_c = 10^7 M_\odot$) and $D = 1h_0$ case. The trapped mass increases rapidly during the formation time of the super-cluster. After the super-cluster has reached its final mass, essentially no late-comers are trapped. To understand the evolution of orbits of stars lying further away than the tidal radius would mean a more in-depth analysis which will be the subject of a later contribution.

In Figure 3 we show the ratio between the mass of the trapped disc stars M_b and the mass of the super-cluster. One clearly sees that the number of trapped disc stars is not negligible. The peak values in all parameter sets are always above 10 per cent of the super-cluster mass M_c . In the model where we added a dynamically cold population, the peak value even reaches approximately 45 per cent. In other words, in the final merger object, a very massive star cluster, one out of three stars was not formed in the starburst which created the object. While the original stars of the super-cluster should all have the same metallicity and age, the trapped stars should show a mix of the populations, metallicities and ages of the underlying disc stars. Most of these stars should stay within the object even if the surrounding disc is destroyed by interactions. The small error-bars in our results indicate that except for some statistical fluctuations of very loosely bound stars our results are not a transient feature as long as the disc potential stays smooth. In the simulations with an initially cold population, the error-bars are larger because the natural heating-up of the cold stars leads to density fluctuations like bars and spiral arms with density contrasts of the order of or even higher than our object, acting as disruptive forces on our super-cluster.

Figure 3 also shows that the peak value arises approximately when the velocity dispersion of the disc stars equals the velocity

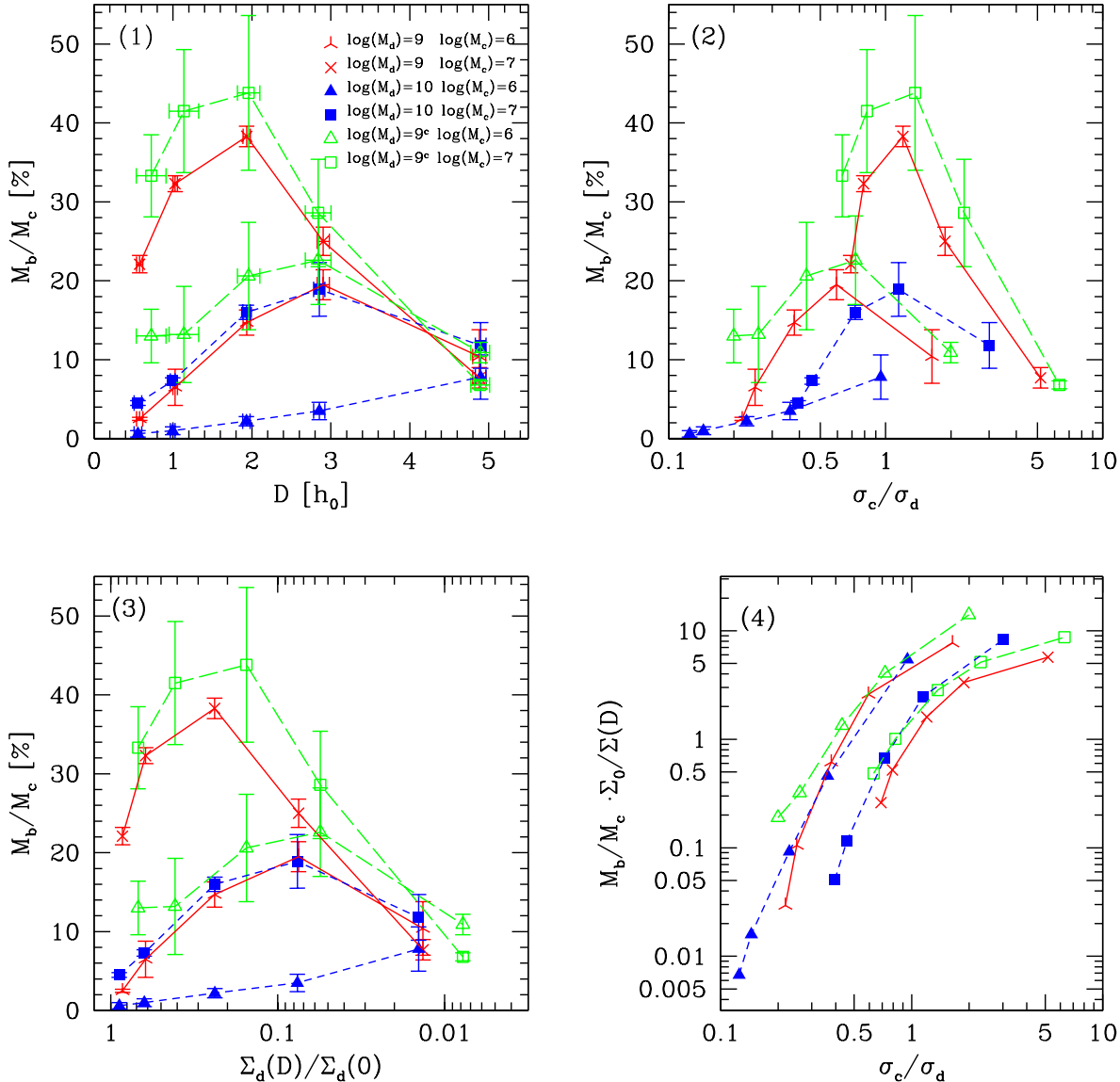


Figure 3. First panel: Ratio between the mass of the trapped disc stars M_b and the initial mass of the super-cluster M_c plotted against the radial distance D to the disc centre in units of the radial scale length of the disc (h_0). Tri-pointed stars ($M_c = 10^6 M_\odot$) and crosses ($M_c = 10^7 M_\odot$) are the results derived in the low mass disc case ($M_d = 10^9 M_\odot$, connected with solid lines, red on-line). Filled triangles ($M_c = 10^6 M_\odot$) and squares ($M_c = 10^7 M_\odot$) are the results of the high mass disc simulations ($M_d = 10^{10} M_\odot$, connected with short dashed lines, blue on-line). Finally, open triangles ($M_c = 10^6 M_\odot$) and open squares ($M_c = 10^7 M_\odot$) denote the results of the low mass disc simulations with 10 % of kinematically cold stars (connected with long dashed lines, green on-line). Second panel shows the same results now plotted against the ratio of the internal velocity dispersion of the cluster complex to the local dispersion of the disc stars. It is clearly visible that the number of trapped stars increases with decreasing velocity dispersion until a ratio of about 1 is reached. Then the number of trapped stars decreases again because now the surface density of the disc stars drops significantly. This is shown in the third panel where the results are plotted against the surface density of the disc measured in units of the central surface density. Finally, in the fourth panel, we multiply our results by the ratio of the surface densities. This panel shows that the turn-over in the previous panels is due to the strong decrease in surface density and may hint that if one has a high density and low velocity dispersion environment, a super-cluster could trap more than its initial mass (see discussion in the main text).

dispersion of the super-cluster. The number of trapped stars then decreases again because the surface density of the disc drops. With adding 10 per cent of kinematically cold stars, i.e. the velocity dispersion of these stars is reduced by a factor of 25, one is able to increase the number of trapped stars by keeping the same surface density (open symbols in Figure 3). But such a cold population is not a stable configuration. Within a few galactic orbits (a

few $\times 0.1 - 1$ Gyr) the stars of the cold sub-population reach the same velocity dispersion as the other disc stars. In the much-more massive Milky Way this is evident in the age-velocity dispersion relation (Kroupa 2002). This time-scale is long compared with the trapping time which is of the order of the formation time of the super-cluster. I.e. the cold sub-population gets trapped preferen-

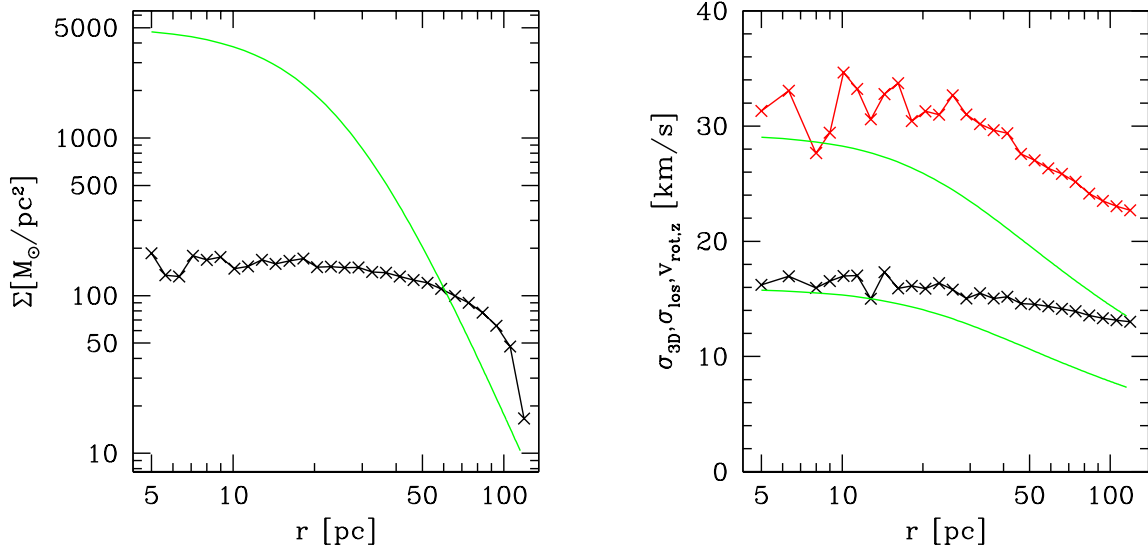


Figure 4. Distribution of the trapped stars for the low-mass disc, massive super-cluster and one scale-length distance simulation. Left panel: Surface density of the trapped stars. Connected crosses show the surface density of the trapped stars, while the solid line (green on-line) shows the surface density profile the pure analytical super-cluster would have (Plummer sphere). Right panel: Upper curves (red and green on-line): 3D-velocity dispersion; lower curves (black and green on-line): line-of-sight velocity dispersion. Connected crosses show the data of the trapped stars while solid lines are the profiles of the analytical super-cluster.

tially and it is possible for it to show an age-spread of about one Gyr when compared to the endemic population.

In the last panel of Figure 3, we show that the turn-over in the ratio of trapped stars is really due to the decreasing surface density. When we divide our results by the ratio between the actual surface density and the central one, the turn-over disappears, showing a mild flattening towards an increasing velocity-dispersion ratio instead (compare panels 2 and 4). It also shows that if the velocity dispersion of the surrounding stars is much lower than the internal dispersion of the super-cluster for a constant surface density, the super-cluster could trap more stars than its initial mass. This may point towards a possible model for ω Cen which has, if the present notion is correct, $M_b/M_c = 70\%/25\% = 2.8$ (Hilker & Richtler 2000); the most metal-rich 5 per cent of its population may then have originated according to the third scenario (accreted gas, Sec. 1).

One may argue that with our setup we create the mass of the super-cluster out of nowhere. This is true but since the mass ratio between the forming cluster and the disc galaxy is small, the adjustment of the host potential through the mass redistribution as a result of cluster formation is a tiny effect. Also the linear increase of the mass of the super-cluster is only the lowest-order approximation. We therefore took one of our setups as described above (small disc, heavy super cluster, one scale-length distance) and changed the way the super-cluster potential grows: the mass is taken to be constant from the beginning of the simulation (mass conservation), but the scale-length (Plummer radius) of the super-cluster is shrunk from a disc scale length (i.e. the mass is distributed over the whole disc extension) to its final value exponentially (slow at the beginning and very fast at the end) in the following way:

$$R_{\text{pl}}(t) = (R_{\text{ini}} - R_{\text{final}}) \cdot (1 - \exp(t - T_{\text{cr}})) + R_{\text{final}}. \quad (3)$$

R_{pl} is the Plummer radius of the growing potential, R_{ini} and R_{final} are its initial ($1h_0$) and final (25 pc) value. T_{cr} denotes the crossing time of the super-cluster. This process models the assembly of a

molecular cloud from the interstellar medium spread throughout a large fraction of the galaxy.

Comparing the results of these two different ways to build-up the super cluster potential shows no difference: While in the first variant we trap $33.2 \pm 1.0\%$ of the initial mass in disc stars, the new build-up version gives us $33.3 \pm 1.0\%$.

We also tested the robustness of our results with linear growth of the potential and different time-scales (1–20 Myr) for the potential to reach its final value and found no significant change of the results.

Finally, we plot the radial profiles of the trapped stars in one of our simulations in Figure 4. The surface density distribution of the trapped stars has a large effective (half-light) radius of about 90 pc. It is much flatter and lower than the distribution of the initial super-cluster. The velocity dispersion of the trapped stars has the same central value as the super-cluster but decreases much more slowly, the trapped stars thereby forming a dynamically hotter population in the outer parts of the final object.

4 CONCLUSIONS

With our suite of simulation, we have shown that it is possible that very massive newborn star clusters or star cluster complexes, which later merge into one massive object, trap a detectable amount of underlying stars of the host galaxy in which they are born. With our choice of parameters, a super-cluster may capture up to one foreign star for every two home stars ($M_b/M_c \approx 0.5$).

We also showed that, in dwarf disc galaxies with exponential profiles, this effect is largest when the velocity dispersions of the super-cluster and the disc stars are comparable. This maximum arises due to the fact that in the outer parts of the disc galaxy, where the velocity dispersion is sufficiently low, the surface density is also very low, i.e. the super-cluster simply does not find enough stars to

6 Fellhauer *et al.*

trap. This is shown in the last panel of Fig. 3. One may also read this panel such that, for a low field velocity dispersion and a constant surface density the super-cluster traps several times its own mass.

The question arises if there are environments with low velocity dispersions (i.e. dynamically cold) which have high densities so that the newborn cluster could even trap several times its own initial mass $M_b/M_c > 2$. These environments are probably not stable dynamically and would heat-up within a few orbital times of the disc, but the time-scale of trapping is much shorter. It is of the order of the formation time of the newborn super-cluster, namely a few Myr. Thus, even in this case the original and captured populations may show substantial age and metallicity differences.

We also expect this effect for massive star clusters born in dSph systems. Even though these systems are dynamically hot given their visible mass, they have velocity dispersions of only about 10 km s^{-1} . If a very massive super-cluster formed in such an object, it would trap a significant amount of old stars. Another dwarf galaxy nearby is the Large Magellanic Cloud (LMC). With a velocity dispersion of about 30 km s^{-1} , we expect that a very massive cluster (say $10^6 M_\odot$) traps a few per cent of its initial mass from the LMC. With better observational data of single stars in the LMC clusters, this could be a measurable effect.

As a final remark, we point out that the surface density distribution of the trapped stars is much flatter than the stars of the initial object and these stars form a dynamically hotter sub-system in the outer parts of the object.

Acknowledgements: MF gratefully acknowledges financial support through DFG-grant KR1635/5-1 and PPARC.

REFERENCES

Bekki K., Norris J.E., 2006, ApJL, 637, 109L
 Binggeli B., Barazza F., Jerjen H., 2000, A&A, 359, 447
 de Blok W.J., Bosma A., 2002, A&A, 385, 816
 Fellhauer M., Kroupa P., Baumgardt H., Bien R., Boily C.M., Spurzem R., Wassmer N., 2000, NewA, 5, 305
 Fellhauer M., 2004, in Schielicke, R.E. (ed.), (2004), Rev.Mod.Astron., 17, 209
 Freeman, K.C., 2001, in Deiters et al. (eds.), Dynamics of Star Clusters and the Milky Way, ASP Conference Series, 228, 43
 Hilker M., Richtler T., 2000, in Noels A., et al. (eds.), From Globular Cluster to Field Star, Proceedings of the 35th Liege International Astrophysic Colloquium, held 5-8 July, 1999
 Ideta M., Makino J., 2004, ApJL, 616, 107L
 Kroupa P., 1998, MNRAS, 300, 200
 Kroupa P., 2002, MNRAS, 330, 707
 van Leeuwen F., Le Poole R.S., Reijns R.A., Freeman K.C., de Zeeuw P.T., 2000, A&A, 360, 472
 Meylan G., Mayor M., Duquennoy A., Dubath P., 1995, A&A, 303, 761
 Meylan G., Sarajedini A., Jablonka P., Djorgovski S.G., Bridges T., Rich R.M., 2001, AJ, 122, 830
 Norris J.E., Da Costa G.S., 1995, ApJ, 447, 680
 Norris J.E., Freeman K.C., Mayor M., Seitzer P., 1997, ApJL, 487, 187L
 Piotto G., Villanova S., Bedin L.R., Gratton R., Cassisi S., Moymany Y., Recio-Blanco A., Lucatello S., Anderson J., King I.R., Pietrinferni A., Carraro G., 2005, ApJ, 621, 777
 Platais I., Wyse R.F.G., Hebb L., Lee Y.-W., Rey S.-C., 2003, ApJL, 591, 127L
 Ree C.H., Yoon S.-J., Rey S.-C., Lee Y.-W., 2002, in van Leeuwen et al. (eds), Omega Centauri, A Unique Window into Astrophysics, ASP Conference Proceedings, 265, 101
 Sollima A., Borissova J., Catelan M., Smith H.A., Minniti D., Cacciari C., Ferraro F.R., 2006, ApJL, 640, 43L
 Spitzer L., 1942, ApJ, 95, 329
 Swaters R.A., van Albada T.S., van der Hulst J.M., Sancisi, R., 2002, A&A, 390, 829
 Swaters R.A., Balcells M., 2002, A&A, 390, 863
 Tsuchiya T., Korchagin V.I., Dinescu D.I., 2004, MNRAS, 350, 1141